EFFECT OF HYDRODYNAMIC DISPERSION ON TRIANGULAR TAYLOR LED PLATFORM RESPONSES

SITI ZAINAB HA
UNIVERSITI TEKNOLOGI PETRONAS

JUNE 2010

CERTIFICATE OF APPROVAL

Effect of Hydrodynamic Coefficients on Triangular Tension Leg Platform (TLP) Responses

by

Mohd. Fahmey Bin Zainudin

A project dissertation submitted to the
Civil Engineering Programme
University Technology of PETRONAS
In partial fulfilment of the requirement for the
Bachelor of Engineering (Hons)
(Civil Engineering)

Approved by,

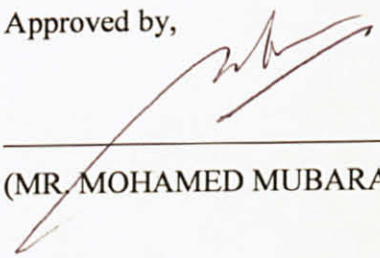

(MR. MOHAMED MUBARAK ABDUL WAHAB)

UNIVERSITY TECHNOLOGY OF PETRONAS
TRONOH, PERAK
Jan 2010

CERTIFICATION OF ORIGINALITY

This is to certify that I am responsible for the work submitted in this project, that the original work is my own except as specified in the references and acknowledgements, and that the original work contained herein have not been undertaken or done by unspecified sources or persons.

MOHD. FAHMEY BIN ZAINUDIN

ABSTRACT

Triangular configuration tension leg platforms (TLPs) are still new in the offshore industry for deep water oil and gas exploration. With its excellent station keeping characteristics for deepwater, this type of platform can be a major consideration for the industry around the world. Instead of square configuration, triangular is used instead because it is more cost effective in term of saving in steel. This study focuses on the effect of the hydrodynamic coefficients which are drag coefficient (C_D) and inertia coefficient (C_M) of triangular tension leg platform responses. The responses that need to be evaluated will be surge and heave responses under the impact wave loads. The Morison's equation will be used to find the forces on each member which is the three hulls and three pontoons. A single-parameter energy spectrum that based on significant wave height or wind speed will be evaluated. By calculating the design parameters of the triangular TLP, Response-Amplitude Operator (RAO) can be obtained and with it the surge and heave responses can be solve analytically. From this analysis, it is indicated that the responses subjected to the three different coefficients give small effect of responses considering three types of members of the triangular tension leg platform which is clean, semi-fouled, and fouled. These prove that the triangular tension leg platform can be designed at any condition of the members.

ACKNOWLEDGNEMENT

First and foremost, pray to God the Al-Mighty for his bless and love, for giving all the strength to complete the final year research project. The project managed to be finished within the time frame. Without the guidance and help from other people, this project would not be able to complete.

I would like to dedicate this project as my gift to my parents who give me a never ending supports and prayers.

My deepest appreciation goes to AP Dr. Kurian V. John, for his expertise, knowledge, ideas, and thoughts. I would also like to thank Mr. Mubarak Abdul Wahab as my supervisor who had been supportive and always motivate for the best outcome of the research. His advices are very valuable for me.

Lastly, thanks to my colleagues for helping me a lot even in difficult situations sometimes.

Thank you.

TABLE OF CONTENTS

LIST OF FIGURES

LIST OF TABLES

CHAPTER 1

INTRODUCTION

1.1 BACKGROUND

Offshore platforms support the exploration and production of oil and gas from beneath the seafloor. The structure should experience minimal movement to provide a stable work station for operation such as drilling and production of oil and it is built out of steel, concrete or a combination of the two. Offshore platforms can be divided into two general categories which are fixed and compliant. Fixed types fully extend to the sea bed and remain in place by a combination of their weight and piles driven into the soil. And the compliant types of platforms are more responsive to external effects where little or no motion of structure can be observed on the fixed types.

The concept of TLP has more attention for deep water applications. It is vertically moored to the seafloor with a bundle arrangement of tensioned tendons attached at each vertical leg. This compliant type of offshore structures are designed so that their dynamic response characteristics are detuned from a wide range of environmental loading conditions in which they are expected to operate. In addition they are designed to allow substantial structural motion during extreme environmental loading condition without damage to the structural integrity of the platform.

Triangular TLP are generally useful for deepwater oil and gas exploration. The tensioned cabling consists of three-tethered leg, each leg being members of multiple parallel cables, terminated at the base of the structure. TLP has a major consideration for deepwater application due to its relative insensitivity with respect to increasing water depth. The saving in steel combined with its excellent station keeping characteristics makes TLP as one of the most cost effective and practical production system for deep-water developments.

1.2 PROBLEM STATEMENT

Triangular TLP has major consideration for deepwater application due to its relative sensitivity with increasing water depth and excellent station keeping characteristics which makes this as a most cost effective and practical production system for deep waters. Hydrodynamic forces on TLPs are evaluated using Morison equation under regular waves. Various nonlinearities arising due to relative velocity term in drag force, change in tether tension due to TLP movement, and set down effect are being considered in the analysis. Response evaluated using varying hydrodynamic coefficients through the water depth and constant coefficients in all activated degrees-of-freedom. The hydrodynamic coefficients also influence the plan dimension of TLP and its site location. [1]

1.3 OBJECTIVES

There are two main objectives for this project:

- To prepare dynamic analysis on the triangular tension leg platform (TLP).
- To determine the effect of hydrodynamic coefficients of a triangular tension leg platform (TLP) due to a random wave.

1.4 SCOPE OF STUDY

- Study in the influence of hydrodynamic coefficients on the nonlinear response behaviour of triangular TLP models under regular waves.
- Study the concepts of TLP in deepwater exploration.
- Study the characteristics and the responses of TLP.
- Perform dynamic analysis of triangular TLP in frequency and time domain.

CHAPTER 2

LITERATURE REVIEW

Model tests of triangular tension leg platform (TLP) concept being developed by Saga Petroleum and Aker Engineering have provided encouraging confirmation that the project is proceeding along the right lines. The model was subjected to a fortnight of tests in Marintek's deepwater tank, including simulated 100-year storms, in simulated water depths up to 1,250 meters. The companies' main points of reference are the Snorre TLP installed on the Norwegian shelf in 1992, and the Heidrun TLP installed on 1995. Snorre has a steel hull, Heidrun a concrete hull, both platforms have four columns and both involved an expensive and lengthy fabrication process. The tether system turned out to be the major high-cost element, and the triangular shape the solution to it. With a three-legged structure, an equal distribution of tension naturally takes place, giving the platform stability which is well suited to rough sea states. There is no need, as there is with four-column TLPs, for a complicated, costly and time-consuming installation operation to achieve the required distribution of tension. The installation of triangular TLP should prove to be much simpler, faster and cheaper than Snorre or Heidrun was. With the triangular concept, there is no need for the diagonal stiffeners required by the four-leg hull and this leads to a 5-15% saving on structural steel. A further round of optimization will take place, with the aim of cutting fabrication time by 50% compared with the time taken to build the Snorre platform. [2]

The study on response behavior of triangular TLP under impact loading done because of the issue that TLPs are often subjected to less probable forces which arise due to collision of ships, ice bergs or any other huge sea creature. Dynamic analysis of the

triangular TLP models was performed under regular waves along with impulse load acting at an angle of 45 degrees at TLP column. The hydrodynamic forces on the TLP model are evaluated using modified Morison equation, based on water particle kinematics arrived at using Stoke's fifth order wave theory. And based on the numerical studies that have been done, it is seen that impulse loading acting on corner column of the triangular TLP model significantly affect its response while that acting on pontoons do not affect the model at all. From this study, hydrodynamic forces can be evaluated for the triangular TLP's responses. [2]

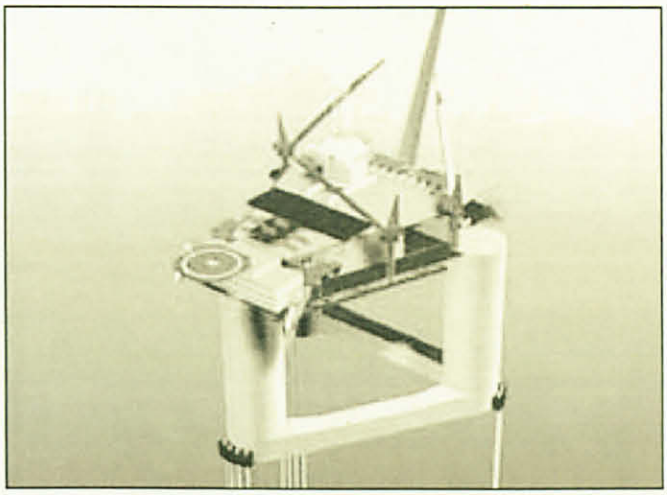

Figure 2.1: The open-space deck is one of three topsides concepts Saga and Aker are studying as part of the triangular TLP project. [3]

Based on the dynamic analysis, dynamic equation of motion has been solved in time-domain by employing Newmark's β numerical integration technique. And based on the numerical study conducted, it is seen that the response evaluated by varying hydrodynamic coefficients through the water depth is significantly smaller in comparison to the response with constant coefficients in all activated degrees-of-freedom. For this study, sway, roll, and yaw degrees-of-freedom are not present due to the unidirectional wave loading. [3]

On the numerical studies conducted on the responses behaviour of triangular TLP models under regular state: [3]

- The variation in the coupled surge responses is significant with varying C_D-C_M values when compared with that of constant coefficients.
- The influence of hydrodynamic coefficients in the wave period of 15s is more in comparison with that of 10s and the variation is nonlinear between the different wave heights with the same wave period (in both the time periods).
- Hydrodynamic coefficients also influence the plan dimension of TLP and its site location (geometric properties). Therefore, it may become essential to estimate the range of the Morison coefficient based on the *Re* and (or) *Kc* even before the preliminary design state of the TLP geometry.
- The coupled responses in all activated degrees-of-freedom are nonlinear.
- For compliant structure like TLP, application of Morison equation without allowance for correctly estimated C_D and C_M values, the response behaviour would be significantly high with that of the expected real behaviour.
- The influence of hydrodynamic coefficients in the response of all activated degrees-of-freedom is significant for the range of their variation selected throughout the water depth.

TLP is a kind of compliant-type offshore platform generally used for deepwater oil of exploration. The increase in cost of fixed offshore structures with increased water depths encouraged the development of compliant-type platforms. The key behind their installation is the minimization of the resistance of structure to environmental loads by making structure flexible. TLP platform is considered as a rigid body having six degrees-of-freedom, namely surge, sway, heave, roll, pitch and yaw. TLP is a hybrid structure with respect to horizontal degrees-of-freedom, it is compliant and behaves like a floating structure. With respect to the vertical degrees-of-freedom, it is stiff and resembles a fixed structure and is not allowed to float freely. The natural periods of the

platform in these degrees-of-freedom vary from 2 to 110 seconds. Surge, sway and yaw have larger periods and heave, roll and pitch have smaller periods. [6]

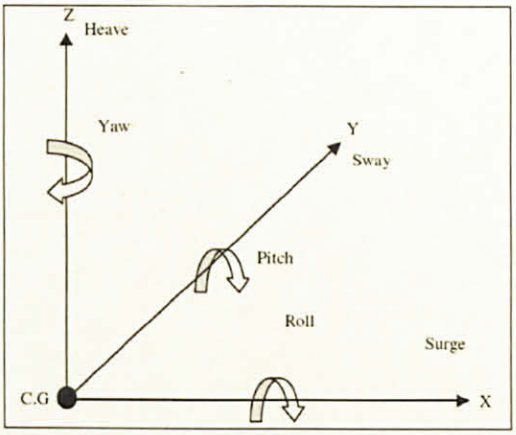

Figure 2.2: Degree-of-Freedom of Triangular TLP

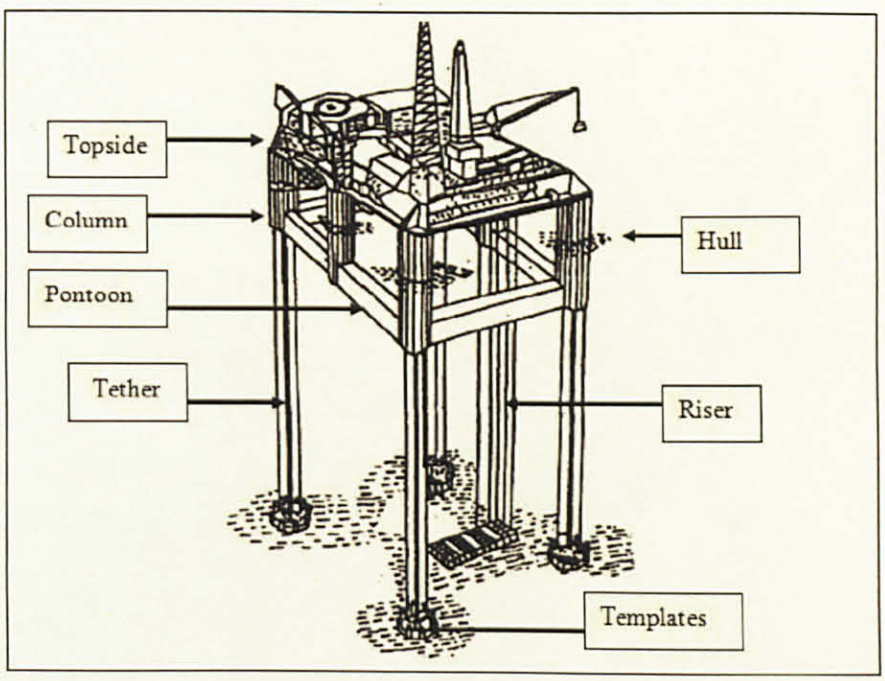

Figure 2.3: TLP Main Components

Some of the TLP advantage compare to other platform are: [6]

- It is much safer in a seismically active zone compared with any other fixed platform.
- Because of the restrained vertical motion of the TLP, it is quite convenient to monitor and maintain the risers, oil wells and tethers.
- A particularly attractive feature of the TLP is the ability to shift any resonance outside the frequency region of the active wave energy.
- It attracts a lesser impact of the wave loading due to its compliant nature and hence can operate even in rough sea.
- The natural frequencies in the main or soft degrees of freedom (surge, sway and yaw) are well below the wave frequencies, thus avoiding the occurrence of resonance and reducing the horizontal motion and hence loading on the tether platform system.
- It is less expensive than the bottom-supported structures, especially in deeper sea.

From the reports based on the prediction of the hydrodynamic forces on a full-scale TLP model, there are two techniques to do the prediction: Computational Fluid Dynamics (CFD), which is based on the solution of the fundamental equations that govern turbulent fluid flow; and by using normal engineering calculations based on force coefficients derived from a design code that always used in the offshore industry. [7]

One of the other study has been done is to validate a new method that can be used by offshore platform designers to estimate the added mass and hydrodynamic damping coefficients of potential TLP's hull configuration since these coefficients are critical to the determination of the TLP's responses particularly to high frequency motions caused by sum-frequency wave forcing. The research further evaluates the component scaling laws for a single vertical cylinder and analyses the effect due to hydrodynamic

interaction. Basically, the hydrodynamic interaction effects are established through a direct comparison between the superposition of individual hull component coefficients and those analyzed directly from complete hull configurations model. The result indicate that from drag contributions to the relative damping matched the expected values scaled based on the diameter (which affect the drag coefficients) to draft dependence. And the inertia coefficients estimated using superposition was slightly lower and more conservative than those measured for the hull configuration. Component scaling proven that it is an effective method by which triangular TLP designers can estimate the hydrodynamic response of a prototype hull in heave. [8]

The Morison equation assumes the force to be composed of inertia and drag forces linearly added together. The components involve an inertia (or mass) coefficient and a drag coefficient which must be determined experimentally. The Morison equation is applicable when the drag force is significant. This is usually the case when a structure is small compared to the water wave length. Morison, *et al.* proposed that the force exerted by unbroken surface waves on a vertical cylindrical pile which extends from the bottom through the free surface is composed of two components, inertia and drag. C_M and C_D are at least functions of *Kc* number, *Re* number, roughness parameters, and interaction parameter. [12]

CHAPTER 3

METHODOLOGY

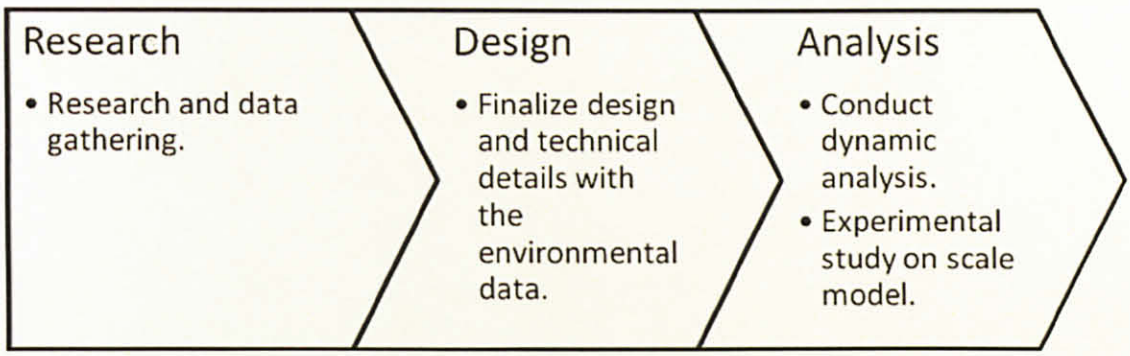

Figure 3.1: Project Methodology Diagram

The above diagram represents the overall flowchart of this project. The three main steps which is research, design and followed by analysis will be further explained in details.

3.1 RESEARCH

Detailed study and research on this topic is collected from internet, journal and book to help better understanding on the dynamic analysis and also the concept of the triangular

TLP. The required data should be gathered is the dimensional data of the triangular TLP and the environmental data.

3.2 DESIGN

This step is where selection of design, technical details and properties of triangular TLP is made. Environmental data also selected for dynamic analysis purposes.

The data for a typical triangular tension leg platform have been collected and several modifications had been made for the study. The environmental data has been taken from PTS 20073 Supplementary. The dimensional, structural and environmental data of the triangular TLP are given as the tables follows:

Table 3.1: Dimensional Data

Section	Diameter (m)	Length (m)	Amount
Column	20	50	3
Pontoon	20	50	3
Tendons	1	965	12 (4 at each column)

Table 3.2: Structural Data

Total mass (tones)	70,000
Total weight (kN)	686,700
Tethers stiffness (kN/m)	100,000
Draught (m)	35

Table 3.3: Environmental Data (Operating Criteria)

Wave	
Significant wave height, H_s (m)	3.6
Zero crossing wave period, T_z (s)	6.6
Peak wave period, T_p (s)	9.3
Individual maximum wave height, H_{max} (m)	6.4
Associated wave period, T_{ass} (s)	8.6
Water depth, d (m)	1000
Ocean Current	
At surface, d (m/s)	1.4
At mid-depth, 0.5 x d (m/s)	1.3
At near seabed, 0.01 x d (m/s)	0.7

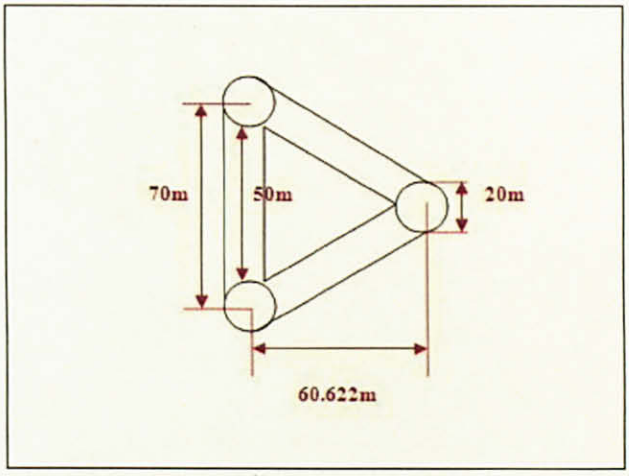

Figure 3.2: Plan Dimensional View

Figure 3.2 show the dimensional side view of the triangular TLP.

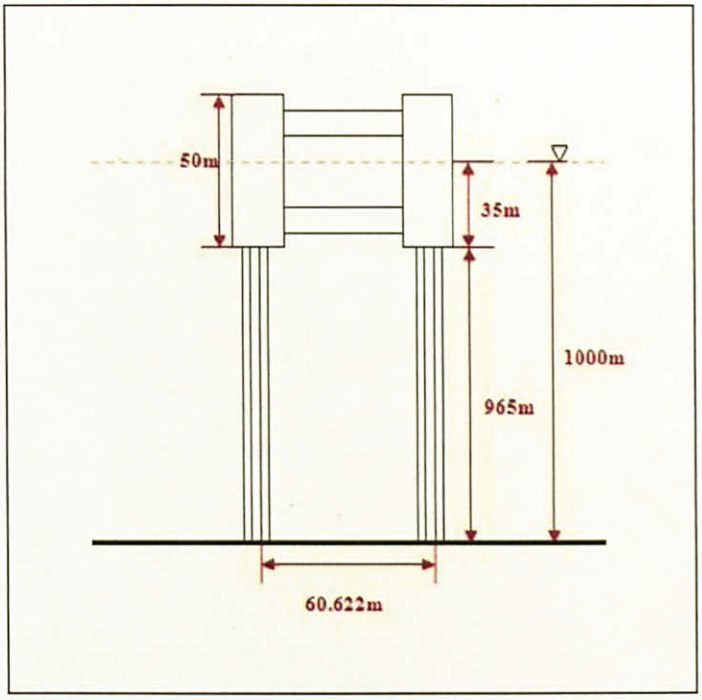

Figure 3.3: Side Dimensional View

Figure 3.3 shows the dimensional side view of the triangular TLP.

3.3 ANALYSIS

For analysis, numerical studies are conducted to highlight the effect of hydrodynamic coefficients C_D and C_M of the triangular TLP responses. Morison equations with Pierson-Moskowitz Spectrum are used to study motion responses acting on the triangular TLP model which are the surge, heave and pitch.

For the purpose of wave forces measurement, Morrison equation is used by implementing the following formulas:

$$df_I = C_M \rho \frac{\pi}{4} D^2 \frac{\partial u}{\partial t} \, ds \qquad [12]$$

where df_I is inertia force on the segment ds of the vertical cylinder, D = cylinder diameter, $\frac{\partial u}{\partial t}$ = local water particle acceleration at the centerline of the cylinder and C_M = inertia coefficient.

$$df_D = \frac{1}{2} C_D \rho D |u| u \, ds \qquad [12]$$

where df_D is drag force on an incremental segment, ds, of the cylinder, u = instantaneous water particle velocity and C_D = drag coefficient.

$$f = C_M A_I \frac{\partial u}{\partial t} + C_D A_D |u| u = df_I + df_D \qquad [12]$$

where f = force per unit length of the vertical cylinder.

The empirical force model proposed by Morison, *et al.* (1950) has been most widely used and accepted in determining forces on thin cylindrical members in an offshore structure. The computation depends on the knowledge of water particle kinematics and empirically determined hydrodynamic coefficients. Sarpakaya and Isaacson (1981) showed that C_D and C_M are functions of Keulegan-Carpenter number (*Kc*), Reynolds number (*Re*), and roughness parameter of the cylinder. Keulegan-Carpenter number (*Kc*) is a measure of water particle orbital amplitude with respect to cylinder diameter, and has been defined in terms of amplitude of the water particle velocity. [1]

The most common used mathematical spectrum model is the Pierson-Moskowitz (1964). It is a single-parameter spectrum that based on significant wave height or wind speed. The energy spectrum is given in terms of a power of the wave frequency, ω. The fetch and duration for this model are considered infinite. [12]

P-M spectrum model is written as

$$S(\omega) = \alpha g^2 \omega^{-5} \exp\left[-0.74\left(\frac{\omega U_W}{g}\right)^{-4}\right] \quad [12]$$

Variance of wave elevation (σ^2) or zeroth moment (m_0) is defined as the area under the spectral curve

$$\sigma^2 = m_0 = \int_0^\infty S(\omega)\, d\omega \quad [12]$$

For the peak frequency

$$H_s = 4\sigma \quad [12]$$

is related to the significant wave height H_s by

$$\omega_0^2 = 0.161 g / H_s \quad [12]$$

The response's amplitude is generally normalized with respect to the amplitude of the wave. Response-Amplitude Operator (RAO) is a function where a normalized response function is constructed for a range of wave frequencies of interest of an offshore structure. It is important to study the overall response of the structure due to a design-wave spectrum since the structure itself is free to move in waves. Its motion could be critical near the resonance of the structure. [12]

The response function at a wave frequency is

$$Response(t) = (RAO)\eta(t) \quad [12]$$

$\eta(t)$ = wave profile as a function of time, t

$$x(t) = \left[\frac{F_a/(H/2)}{[(K-m\omega^2)^2+(C\omega)^2]^{1/2}}\right]\eta_\beta(t) \quad [12]$$

β = phase difference between $x(t)$ and $\eta(t)$

$$RAO = \left[\frac{F_a/(H/2)}{[(K-m\omega^2)^2+(C\omega)^2]^{1/2}}\right]$$

The motion spectrum in terms of wave spectrum and an RAO is

$$S_x(\omega) = \left[\frac{F_a/(H/2)}{[(K-m\omega^2)^2+(C\omega)^2]^{1/2}}\right]^2 S(\omega) \quad [12]$$

Thus, with the relations above, the motion-response spectrum obtained.

TLPs are comprised of slender members whose diameter is small relative to the incident wavelength. Therefore, the wave train remains relatively unaffected outside the immediate vicinity of the member. Hence, flow separation is important other than the wave diffraction. As given by Isaacson (1983), for the structures in this flow separation regime, the wave forces are generally computed by Morison equation which gives the force per unit length on the section of the cylinder. [1]

The three variations of hydrodynamic coefficients used in this analysis are:

i. Clean: Cd=0.65, Cm=1.6
ii. Semi-fouled: Cd=0.85, Cm=1.4
iii. Fouled members: Cd=1.05, Cm=1.2

By using data from conceptual design, Response-Amplitude Operators (RAO) can be obtained. The RAO will give theoretical value of surge, heave and pitch responses.

The tools or software required in this analysis are:

- Microsoft Excel
  - To tabulate and calculate the data.
  - To generate the spectrum models.
  - To analyze the data such as to find the significance difference.

CHAPTER 4

RESULTS AND DISCUSSIONS

4.1 ANALYSIS ON WAVE SPECTRUM

A graph of S(f) versus frequency, f is plotted as in Figure 4.1. Wave spectral density S(f) value can be obtained by means of varying frequency, ranging from 0.005 Hz to 0.395 Hz with an interval 0.01.

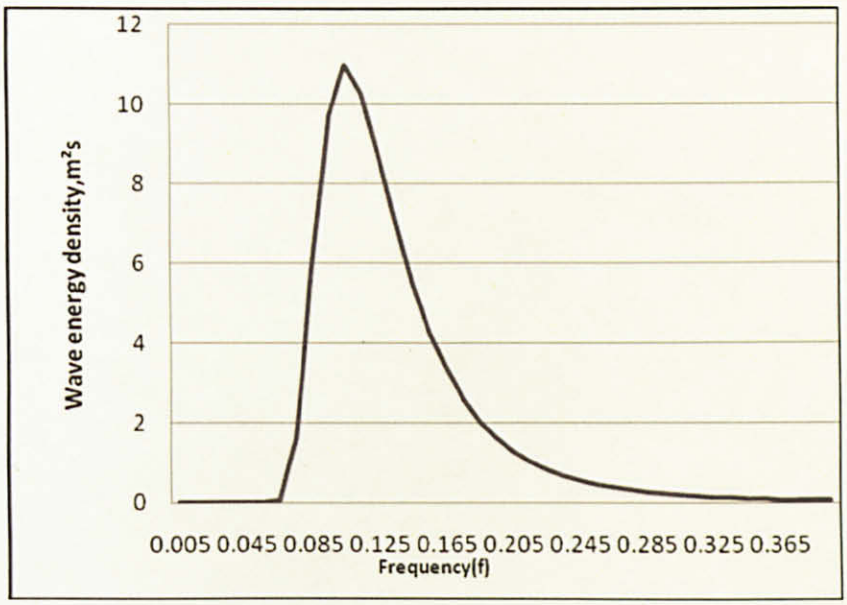

Figure 4.1: Graph of Wave Energy Density Spectrum

Based on Figure 4.1, it is observed that the maximum value of wave energy density is located at peak frequency, f_o = 0.105 Hz. The shape of the spectrum generally rises sharply at low frequency end to a maximum value and decreases gradually with increasing frequency.

4.2 ANALYSIS OF WAVE TIME SERIES

The surface water elevation or the wave profile can be obtained from the wave spectrum energy graph. The range of frequency is taken from 0.005 Hz to 0.395 Hz. *n* values were taken from random numbers, RN which range randomly from 0 to 1. Peak frequency, f_0 is calculated and the value is 0.110 Hz. The assumption for significant wave height is 3.6m. Based on figure 4.2, Range of time applied for the analysis were taken from t=0s to t=100s. The highest elevation is 2.18m at t=3s while the lowest elevation is -2.01m at t=7s.

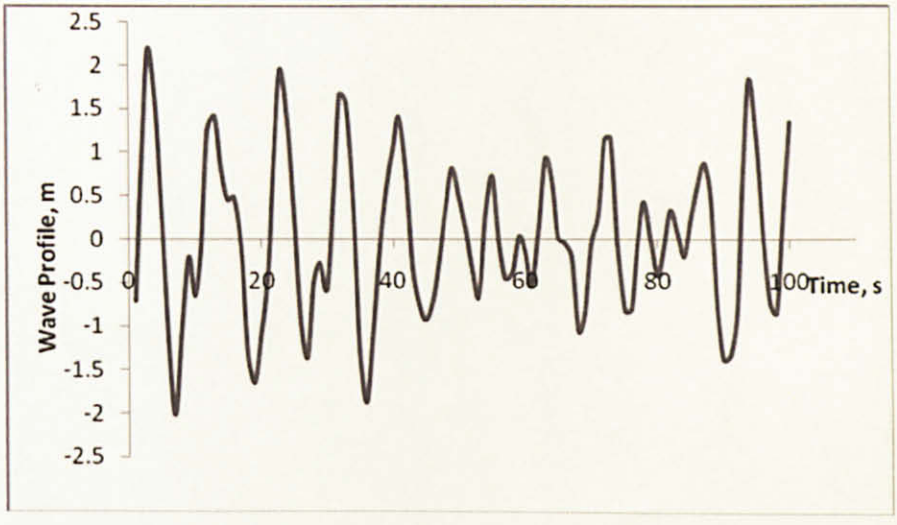

Figure 4.2: Graph of Wave Profile

4.3 SURGE ANALYSIS

Mass of surge, M_{SURGE} = Mass, M + Added Mass, M_{ADD}

= 70,000,000 kg + 49,600,967 kg

= 119,600,967 kg

Buoyant Force, F_B = 947,395,174 N

Tethers Tension, T = Buoyant Force, F_B – Structure Weight in Air, W

= 947,395,174 N – 686,700,000 N

= 260,695,174 N

K_{SURGE} = Tethers Tension, T / Tethers Length, L

= 260,695,174 N / 965m

= 270,150.439 N/m

Damping Coefficient, C $= 2\zeta(K_{SURGE} M_{SURGE})^{1/2}$

$= 2(0.01)(270,150.439 \times 119,600,967)^{1/2}$

= 113,684

The surge parameters will be as attached in Appendix.

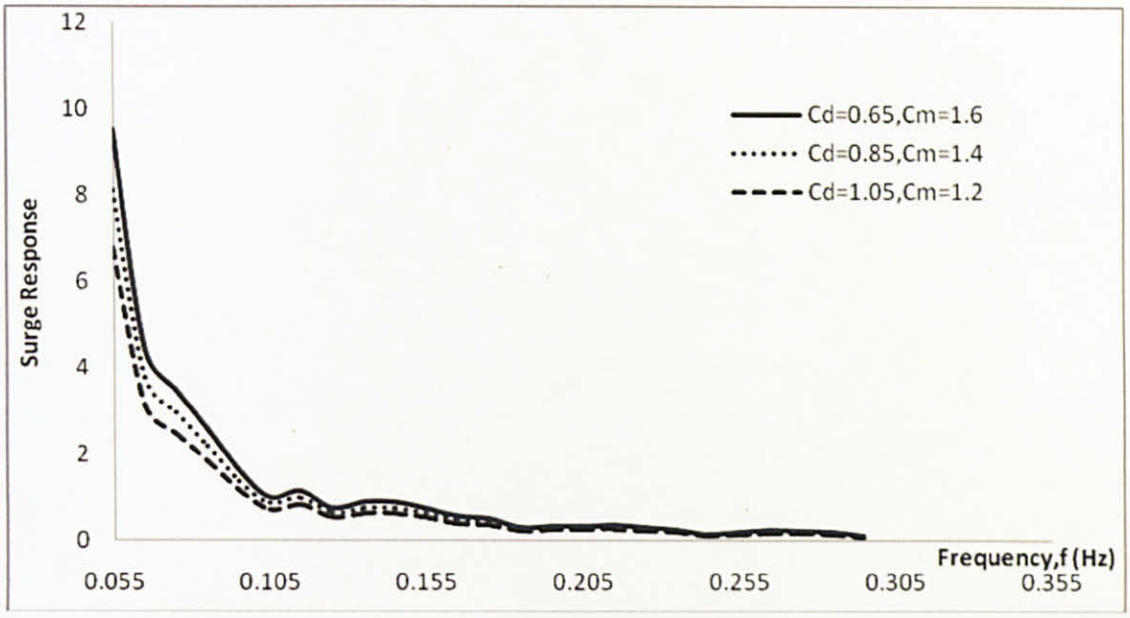

Figure 4.3: Graph of RAO_{SURGE} Subjected to Different Hydrodynamic Coefficients

Table 4.1: Maximum Surge RAO

Members	Max Surge RAO
Clean	9.54
Semi-fouled	8.11
Fouled	6.77

Figure 4.3 shows the surge spectrum RAOSURGE and from table 4.1 clean members has the highest maximum surge RAO at the lowest frequency (0.055 Hz).

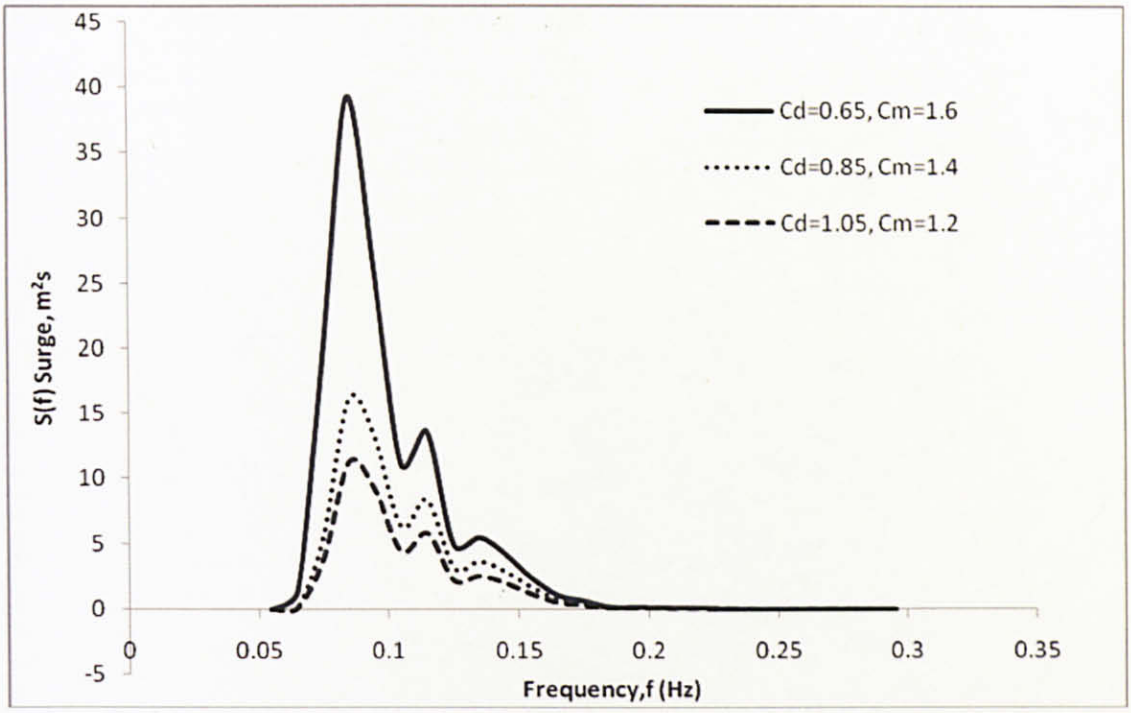

Figure 4.4: Graph of Surge Spectrum Subjected to Different Hydrodynamic Coefficients

Table 5.2: Maximum Surge Energy

Members	Max Energy (m^2s)
Clean	39.16
Semi-fouled	16.11
Fouled	11.24

Figure 4.4 shows that the spectrum is affected by the varying hydrodynamic coefficients. From Table 4.2, the highest response observed is the clean members while the lowest will be the fouled members. The maximum peak for the clean member is at 0.085 Hz.

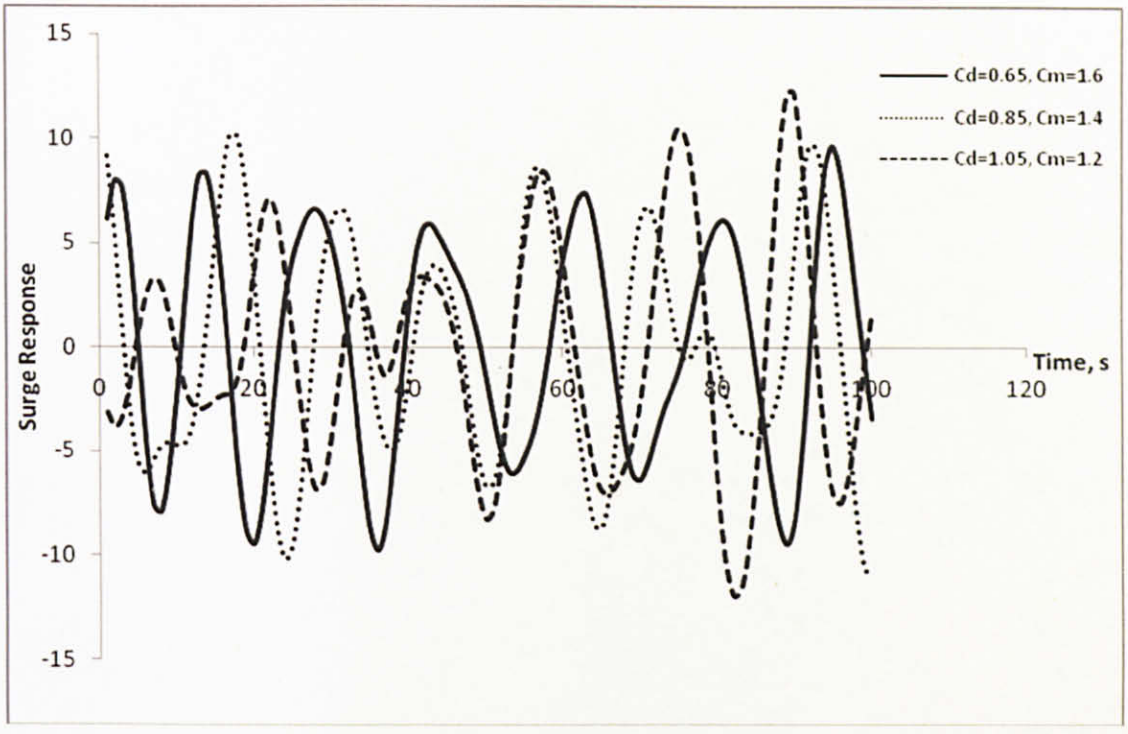

Figure 4.5: Graph of Surge Response Subjected to Different Hydrodynamic Coefficients

Table 6.3: Maximum Surge Response

Members	Max Response (m)
Clean	9.73
Semi-fouled	10.14
Fouled	12.15

From figure 4.5 and based on Table 4.3, the fouled member gives the maximum surge response value which is moving 12.15m to the right since it is positive at t=89s.

4.4 HEAVE ANALYSIS

Mass of surge, M_{HEAVE} = Mass, M + Added Mass, M_{ADD}

= 70,000,000 kg + 25,761,075 kg

= 95,761,075 kg

K_{HEAVE} = 309,473,951.7 N/m

Damping Coefficient, C = 3,442,996.271

The heave parameters will be as attached in Appendix.

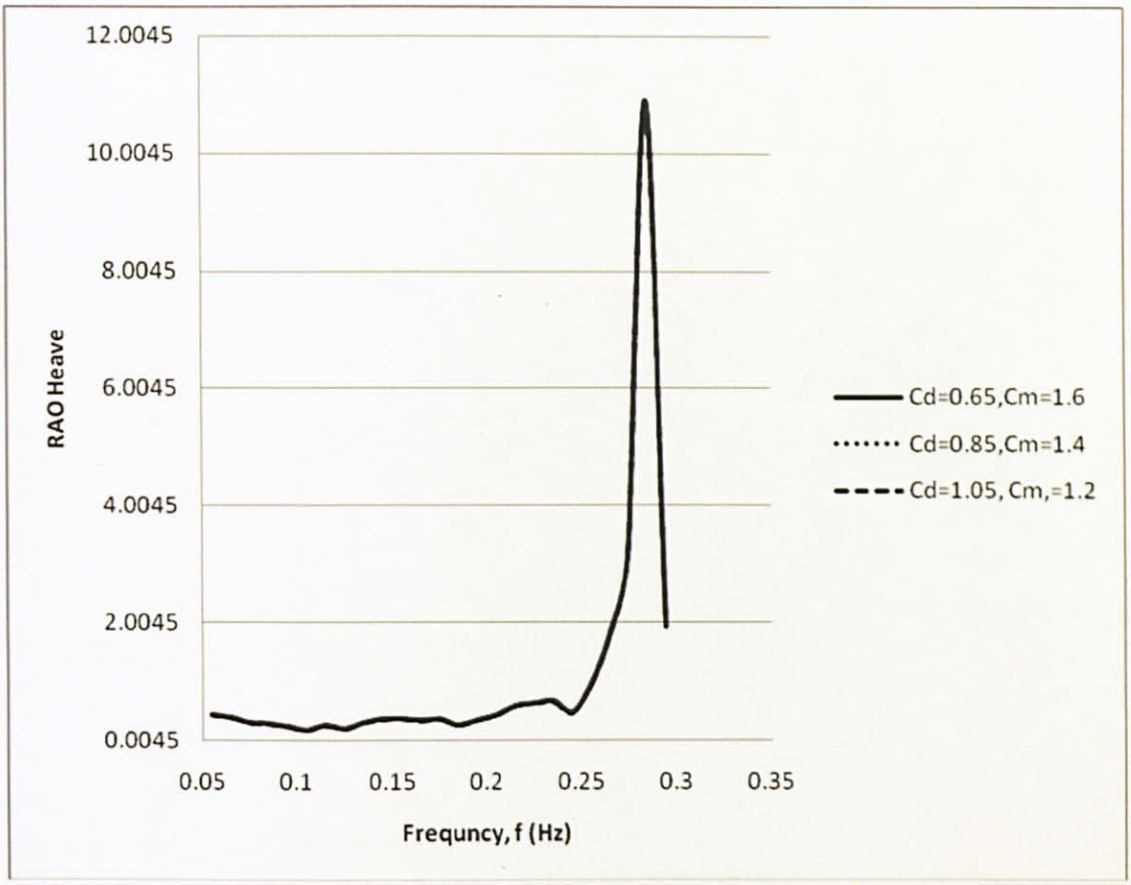

Figure 4.6: Graph of RAO_{HEAVE} Subjected to Different Hydrodynamic Coefficients

Table 7.4: Maximum Heave RAO

Members	Max Heave RAO
Clean	10.79
Semi-fouled	10.79
Fouled	10.79

Figure 4.6 and Table 4.4 shows that varying hydrodynamic coefficients do not affect the RAO_{HEAVE} (heave responses). From this graph, the highest response is at 0.285 Hz.

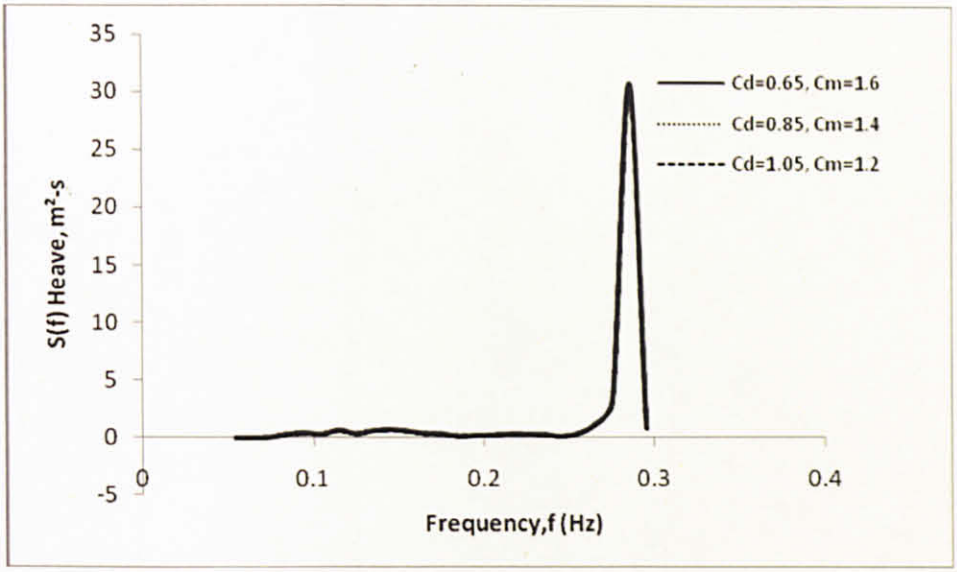

Figure 4.7: Graph of Heave Spectrum Subjected to Different Hydrodynamic Coefficients

Table 8.5: Maximum Heave Energy

Members	Max Energy (m^2s)
Clean	30.12
Semi-fouled	30.12
Fouled	30.12

From Figure 4.7 and Table 4.5, this also tells that the hydrodynamic coefficient slightly affect the heave spectrum. The result shows the highest spectrum is at 0.285 Hz.

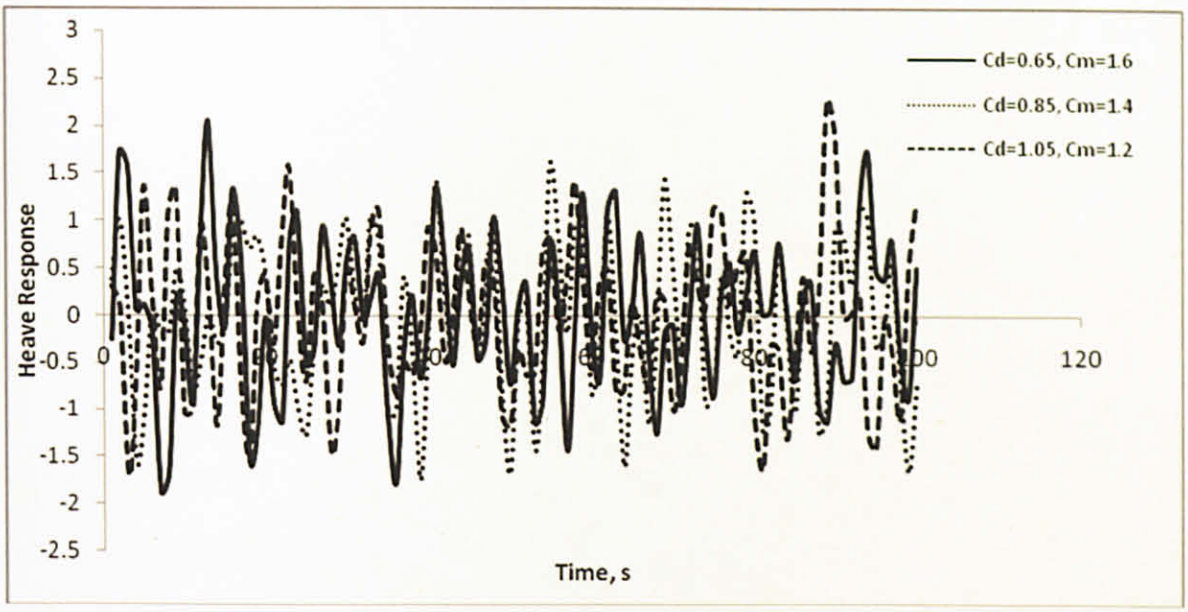

Figure 4.8: Graph of Heave Response Subjected to Different Hydrodynamic Coefficients

Table 9.6: Maximum Heave RAO

Members	Max Response (m)
Clean	2.05
Semi-fouled	1.75
Fouled	2.27

Figure 4.8 and Table 4.6 shows the heave responses subjected to varying hydrodynamic coefficient. From the graph, the maximum positive response is 2.3m at t=89s for fouled member. And the maximum negative response is -1.87m at t=7s for clean member.

CHAPTER 5

CONCLUSION AND RECOMMENDATION

All the objectives are achieved in the end. A detailed research has been done from journals to books from many different authors from around the world to study about the gap of knowledge on this topic. The responses of triangular tension leg platform by the effect of hydrodynamic coefficient can be calculated mathematically under random waves by using certain formulas. Based on the responses on surge, clean member has the lowest response which is 9.73m and fouled member has the highest which is 12.15m. Based on the responses on heave, semi-fouled member has the lowest response which is 1.75m and fouled member has the highest which is 2.27m Hydrodynamic coefficients do not effect much on vertical motion (heave).

Hydrodynamic coefficients are considered in designing the triangular TLP. The analysis indicated that the responses subjected to the three different coefficients give small effect of responses considering three types of members of the triangular tension leg platform which is clean, semi-fouled, and fouled. These prove that the triangular tension leg platform can be designed at any condition of the members.

For future research, it is recommended that this study include a real scale model to verify the theoretical data which is the responses. This is one of the important parts in designing a triangular tension leg platform.

CHAPTER 6

ECONOMIC BENEFITS

In recent years, the demand for affordable technology has led to a considerable effort intended to reduce the overall development cost of offshore platform. Triangular tension leg platform is an alternative solution to normal square tension leg platform. Sizing strategy, details of configurations developed, and sensitivity of cost estimates needed.

The economic value this triangular tension leg platform for this project in the industry is more cost effective than the normal square TLP. This is because of the savings in steels' cost for the platform. One of the reasons to develop this platform for the offshore industry in deepwater is because of the economic advantages.

By considering the hydrodynamic coefficients to the design, ocean engineer later on can save more steel cost for the structure in their design by choosing the cost effective shape of the hull or the pontoon. This shape will affect the hydrodynamic coefficients (drag coefficient).

REFERENCES

[1] Wang Tao, Zou Jun, 2006. *Hydrodynamics in Deepwater TLP Tendon Design.* Conference of Global Chinese Scholars on Hydrodynamics.

[2] S. Chandrasekaran, A.K. Jain, A. Gupta, A. Srivastava, 2006. *Response Behaviour of Triangular Tension Leg Platform Under Impact Loading.* Journal of Ocean Engineering 34, 45-53.

[3] S. Chandrasekaran, A.K. Jain, N.R. Chandak, 2004. *Influence of Hydrodynamic Coefficients in the Response Behavior of Triangular TLPs in Regular Waves.* Journal of Ocean Engineering 31, 2319-2342.

[4] Muhittin Söylemez, Oğuz Yılmaz, 2003. *Hydrodynamic Design of a TLP type offloading platform.* Journal of Ocean Engineering 30, 1269-1282.

[5] S. Chandrasekaran, A.K. Jain, 2002. *Dynamic behaviour of a square and triangular offshore tension leg platform under regular wave loads.* Journal of Ocean Engineering 29, 279-313.

[6] S. Chandrasekaran, A.K. Jain, 2001. *Triangular Configuration Tension Leg Platform Behaviour Under Random Sea Wave Loads.* Journal of Ocean Engineering 29, 1895-1928.

[7] B.A. Younis, P. Teigen, V.P. Przulj, 2001. *Estimating the hydrodynamic forces on a mini TLP with a computational fluid dynamics and design-code techniques.* Journal of Ocean Engineering 28, 585-602.

[8] James J. O' Kane, Armin W. Troesch, Krish P. Thiagarajan, 2000. *Hull Component Interaction and Scaling for TLP Hydrodynamic Coefficients.* Journal of Ocean Engineering 29, 513-532.

[9] R. Burrows, R.G. Tickell, D. Hames & G. Najafian, 1997. *Morison Wave Force Coefficients for Application to Random Seas.* Journal of Applied Ocean Research 19, 183-199.

[10] Anonymous, 1996. <*http://www.offshore-mag.com/index/article-display/23509/s-articles/s-offshore/s-volume-56/s-issue-4/s-news/s-general-interest/s-norway-benefits-stack-up-for-triangular-tlp.html*>. Offshore Magazine Issue 4.

[11] Zeki Demirbilek, 1989. *Tension Leg Platform: A State of the Art Review.* American Society of Civil Engineers.

[12] S.K. Chakrabarti, 1987. *Hydrodynamics of Offshore Strutures.* WIT Press.

APPENDICES

EXAMPLES OF EXCELS' CALCULATIONS

x	t	L_o	L	k	ω	θ	cos θ	sin θ	s	cosh ks	sinh ks	cosh kd	sinh kd	u water pa	u current (	total u (m/s)	U dot (m/s²)	Fd (N/m)	Fi (N/m)	Total horizontal force (N/m)
-20.207	0	33.776	33.776	0.186	1.351	-3.7585	-0.81567	0.578517	999.5	2.05E+23	2.05E+23	2.11E+23	2.11E+23	-1.85581	1.3999	-0.455908924	0.96164795	2.295E+04	4.955E+05	5.184E+05
-20.207	0	33.776	33.776	0.186	1.351	-3.7585	-0.81567	0.578517	998.5	1.95E+23	1.95E+23	2.11E+23	2.11E+23	-1.75755	1.3997	-0.357849797	0.91073177	2.058E+04	4.692E+05	4.898E+05
-20.207	0	33.776	33.776	0.186	1.351	-3.7585	-0.81567	0.578517	997.5	1.84E+23	1.84E+23	2.11E+23	2.11E+23	-1.66449	1.3995	-0.264993176	0.86251145	1.846E+04	4.444E+05	4.628E+05
-20.207	0	33.776	33.776	0.186	1.351	-3.7585	-0.81567	0.578517	996.5	1.75E+23	1.75E+23	2.11E+23	2.11E+23	-1.57636	1.3993	-0.177063605	0.81684424	1.656E+04	4.209E+05	4.374E+05
-20.207	0	33.776	33.776	0.186	1.351	-3.7585	-0.81567	0.578517	995.5	1.65E+23	1.65E+23	2.11E+23	2.11E+23	-1.4929	1.3991	-0.093800211	0.77359495	1.485E+04	3.986E+05	4.134E+05
-20.207	0	33.776	33.776	0.186	1.351	-3.7585	-0.81567	0.578517	994.5	1.57E+23	1.57E+23	2.11E+23	2.11E+23	-1.41386	1.3989	-0.014955936	0.73263558	1.332E+04	3.775E+05	3.908E+05
-20.207	0	33.776	33.776	0.186	1.351	-3.7585	-0.81567	0.578517	993.5	1.48E+23	1.48E+23	2.11E+23	2.11E+23	-1.339	1.3987	0.059703198	0.69384488	1.195E+04	3.575E+05	3.694E+05
-20.207	0	33.776	33.776	0.186	1.351	-3.7585	-0.81567	0.578517	992.5	1.4E+23	1.4E+23	2.11E+23	2.11E+23	-1.2681	1.3985	0.130398781	0.65710802	1.071E+04	3.386E+05	3.493E+05
-20.207	0	33.776	33.776	0.186	1.351	-3.7585	-0.81567	0.578517	991.5	1.33E+23	1.33E+23	2.11E+23	2.11E+23	-1.20096	1.3983	0.197340671	0.62231626	9.609E+03	3.206E+05	3.302E+05
-20.207	0	33.776	33.776	0.186	1.351	-3.7585	-0.81567	0.578517	990.5	1.26E+23	1.26E+23	2.11E+23	2.11E+23	-1.13737	1.3981	0.260727613	0.58936661	8.619E+03	3.037E+05	3.123E+05
-20.207	0	33.776	33.776	0.186	1.351	-3.7585	-0.81567	0.578517	989.5	1.19E+23	1.19E+23	2.11E+23	2.11E+23	-1.07715	1.3979	0.32074783	0.55816154	7.730E+03	2.876E+05	2.953E+05
-20.207	0	33.776	33.776	0.186	1.351	-3.7585	-0.81567	0.578517	988.5	1.13E+23	1.13E+23	2.11E+23	2.11E+23	-1.02012	1.3977	0.377579581	0.52860868	6.933E+03	2.724E+05	2.793E+05
-20.207	0	33.776	33.776	0.186	1.351	-3.7585	-0.81567	0.578517	987.5	1.07E+23	1.07E+23	2.11E+23	2.11E+23	-0.96611	1.3975	0.431391683	0.50062055	6.219E+03	2.579E+05	2.641E+05
-20.207	0	33.776	33.776	0.186	1.351	-3.7585	-0.81567	0.578517	986.5	1.01E+23	1.01E+23	2.11E+23	2.11E+23	-0.91496	1.3973	0.482344018	0.4741143	5.577E+03	2.443E+05	2.499E+05
-20.207	0	33.776	33.776	0.186	1.351	-3.7585	-0.81567	0.578517	985.5	9.59E+22	9.59E+22	2.11E+23	2.11E+23	-0.86651	1.3971	0.530588	0.44901147	5.002E+03	2.313E+05	2.363E+05
-20.207	0	33.776	33.776	0.186	1.351	-3.7585	-0.81567	0.578517	984.5	9.09E+22	9.09E+22	2.11E+23	2.11E+23	-0.82063	1.3969	0.57626703	0.42523775	4.487E+03	2.191E+05	2.236E+05
-20.207	0	33.776	33.776	0.186	1.351	-3.7585	-0.81567	0.578517	983.5	8.61E+22	8.61E+22	2.11E+23	2.11E+23	-0.77718	1.3967	0.619516912	0.40272278	4.024E+03	2.075E+05	2.115E+05
-20.207	0	33.776	33.776	0.186	1.351	-3.7585	-0.81567	0.578517	982.5	8.15E+22	8.15E+22	2.11E+23	2.11E+23	-0.73603	1.3965	0.660466262	0.3813999	3.609E+03	1.965E+05	2.001E+05
-20.207	0	33.776	33.776	0.186	1.351	-3.7585	-0.81567	0.578517	981.5	7.72E+22	7.72E+22	2.11E+23	2.11E+23	-0.69706	1.3963	0.699236886	0.361206	3.237E+03	1.861E+05	1.893E+05
-20.207	0	33.776	33.776	0.186	1.351	-3.7585	-0.81567	0.578517	980.5	7.31E+22	7.31E+22	2.11E+23	2.11E+23	-0.66016	1.3961	0.735944141	0.3420813	2.904E+03	1.762E+05	1.792E+05
-20.207	0	33.776	33.776	0.186	1.351	-3.7585	-0.81567	0.578517	979.5	6.92E+22	6.92E+22	2.11E+23	2.11E+23	-0.6252	1.3959	0.770697275	0.32396919	2.604E+03	1.669E+05	1.695E+05
-20.207	0	33.776	33.776	0.186	1.351	-3.7585	-0.81567	0.578517	978.5	6.56E+22	6.56E+22	2.11E+23	2.11E+23	-0.5921	1.3957	0.803599753	0.30681606	2.336E+03	1.581E+05	1.604E+05
-20.207	0	33.776	33.776	0.186	1.351	-3.7585	-0.81567	0.578517	977.5	6.21E+22	6.21E+22	2.11E+23	2.11E+23	-0.56075	1.3955	0.83474956	0.29057114	2.095E+03	1.497E+05	1.518E+05
-20.207	0	33.776	33.776	0.186	1.351	-3.7585	-0.81567	0.578517	976.5	5.88E+22	5.88E+22	2.11E+23	2.11E+23	-0.53106	1.3953	0.864239496	0.27518633	1.879E+03	1.418E+05	1.437E+05
-20.207	0	33.776	33.776	0.186	1.351	-3.7585	-0.81567	0.578517	975.5	5.57E+22	5.57E+22	2.11E+23	2.11E+23	-0.50294	1.3951	0.892157446	0.26061609	1.685E+03	1.343E+05	1.360E+05
-20.207	0	33.776	33.776	0.186	1.351	-3.7585	-0.81567	0.578517	974.5	5.27E+22	5.27E+22	2.11E+23	2.11E+23	-0.47631	1.3949	0.91858664	0.24681731	1.512E+03	1.272E+05	1.287E+05
-20.207	0	33.776	33.776	0.186	1.351	-3.7585	-0.81567	0.578517	973.5	4.99E+22	4.99E+22	2.11E+23	2.11E+23	-0.45109	1.3947	0.943605904	0.23374912	1.356E+03	1.204E+05	1.218E+05
-20.207	0	33.776	33.776	0.186	1.351	-3.7585	-0.81567	0.578517	972.5	4.73E+22	4.73E+22	2.11E+23	2.11E+23	-0.42721	1.3945	0.967289888	0.22137286	1.216E+03	1.141E+05	1.153E+05
-20.207	0	33.776	33.776	0.186	1.351	-3.7585	-0.81567	0.578517	971.5	4.48E+22	4.48E+22	2.11E+23	2.11E+23	-0.40459	1.3943	0.989709292	0.20965188	1.091E+03	1.080E+05	1.091E+05
-20.207	0	33.776	33.776	0.186	1.351	-3.7585	-0.81567	0.578517	970.5	4.24E+22	4.24E+22	2.11E+23	2.11E+23	-0.38317	1.3941	1.010931072	0.19855148	9.782E+02	1.023E+05	1.033E+05
-20.207	0	33.776	33.776	0.186	1.351	-3.7585	-0.81567	0.578517	969.5	4.02E+22	4.02E+22	2.11E+23	2.11E+23	-0.36288	1.3939	1.031018637	0.18803882	8.773E+02	9.688E+04	9.776E+04
-20.207	0	33.776	33.776	0.186	1.351	-3.7585	-0.81567	0.578517	968.5	3.81E+22	3.81E+22	2.11E+23	2.11E+23	-0.34367	1.3937	1.05003204	0.17808277	7.869E+02	9.175E+04	9.254E+04
-20.207	0	33.776	33.776	0.186	1.351	-3.7585	-0.81567	0.578517	967.5	3.6E+22	3.6E+22	2.11E+23	2.11E+23	-0.32547	1.3935	1.068028156	0.16865386	7.058E+02	8.689E+04	8.760E+04
-20.207	0	33.776	33.776	0.186	1.351	-3.7585	-0.81567	0.578517	966.5	3.41E+22	3.41E+22	2.11E+23	2.11E+23	-0.30824	1.3933	1.085060845	0.15972418	6.330E+02	8.229E+04	8.293E+04
-20.207	0	33.776	33.776	0.186	1.351	-3.7585	-0.81567	0.578517	965.5	3.23E+22	3.23E+22	2.11E+23	2.11E+23	-0.29192	1.3931	1.101181119	0.15126729	5.678E+02	7.794E+04	7.850E+04

x	t	L_o	L	k	ω	θ	cos θ	sin θ	s	cosh ks	sinh ks	cosh kd	sinh kd	u water pa	u current (	total u (m/	U dot (m/s	Fd (N/m)	Fi (N/m)	Total horizontal force (N/
40.41	9	33.776	33.776	0.186	1.351	-4.6427	-0.06959	0.997575	999.5	2.05E+23	2.05E+23	2.11E+23	2.11E+23	-0.15834	1.3999	1.241563	1.658234	1.670E+02	8.544E+05	8.545E+05
40.41	9	33.776	33.776	0.186	1.351	-4.6427	-0.06959	0.997575	998.5	1.95E+23	1.95E+23	2.11E+23	2.11E+23	-0.14995	1.3997	1.249747	1.570436	1.498E+02	8.091E+05	8.093E+05
40.41	9	33.776	33.776	0.186	1.351	-4.6427	-0.06959	0.997575	997.5	1.84E+23	1.84E+23	2.11E+23	2.11E+23	-0.14201	1.3995	1.257486	1.487286	1.344E+02	7.663E+05	7.664E+05
40.41	9	33.776	33.776	0.186	1.351	-4.6427	-0.06959	0.997575	996.5	1.75E+23	1.75E+23	2.11E+23	2.11E+23	-0.13449	1.3993	1.264805	1.408539	1.205E+02	7.257E+05	7.258E+05
40.41	9	33.776	33.776	0.186	1.351	-4.6427	-0.06959	0.997575	995.5	1.65E+23	1.65E+23	2.11E+23	2.11E+23	-0.12737	1.3991	1.271726	1.333961	1.081E+02	6.873E+05	6.874E+05
40.41	9	33.776	33.776	0.186	1.351	-4.6427	-0.06959	0.997575	994.5	1.57E+23	1.57E+23	2.11E+23	2.11E+23	-0.12063	1.3989	1.27827	1.263333	9.695E+01	6.509E+05	6.510E+05
40.41	9	33.776	33.776	0.186	1.351	-4.6427	-0.06959	0.997575	993.5	1.48E+23	1.48E+23	2.11E+23	2.11E+23	-0.11424	1.3987	1.284457	1.196443	8.695E+01	6.164E+05	6.165E+05
40.41	9	33.776	33.776	0.186	1.351	-4.6427	-0.06959	0.997575	992.5	1.4E+23	1.4E+23	2.11E+23	2.11E+23	-0.10819	1.3985	1.290306	1.133095	7.799E+01	5.838E+05	5.839E+05
40.41	9	33.776	33.776	0.186	1.351	-4.6427	-0.06959	0.997575	991.5	1.33E+23	1.33E+23	2.11E+23	2.11E+23	-0.10247	1.3983	1.295835	1.073102	6.995E+01	5.529E+05	5.530E+05
40.41	9	33.776	33.776	0.186	1.351	-4.6427	-0.06959	0.997575	990.5	1.26E+23	1.26E+23	2.11E+23	2.11E+23	-0.09704	1.3981	1.30106	1.016284	6.274E+01	5.236E+05	5.237E+05
40.41	9	33.776	33.776	0.186	1.351	-4.6427	-0.06959	0.997575	989.5	1.19E+23	1.19E+23	2.11E+23	2.11E+23	-0.0919	1.3979	1.305998	0.962475	5.627E+01	4.959E+05	4.959E+05
40.41	9	33.776	33.776	0.186	1.351	-4.6427	-0.06959	0.997575	988.5	1.13E+23	1.13E+23	2.11E+23	2.11E+23	-0.08704	1.3977	1.310664	0.911515	5.047E+01	4.696E+05	4.697E+05
40.41	9	33.776	33.776	0.186	1.351	-4.6427	-0.06959	0.997575	987.5	1.07E+23	1.07E+23	2.11E+23	2.11E+23	-0.08243	1.3975	1.315072	0.863253	4.527E+01	4.448E+05	4.448E+05
40.41	9	33.776	33.776	0.186	1.351	-4.6427	-0.06959	0.997575	986.5	1.01E+23	1.01E+23	2.11E+23	2.11E+23	-0.07806	1.3973	1.319236	0.817547	4.060E+01	4.212E+05	4.213E+05
40.41	9	33.776	33.776	0.186	1.351	-4.6427	-0.06959	0.997575	985.5	9.59E+22	9.59E+22	2.11E+23	2.11E+23	-0.07393	1.3971	1.32317	0.77426	3.642E+01	3.989E+05	3.990E+05
40.41	9	33.776	33.776	0.186	1.351	-4.6427	-0.06959	0.997575	984.5	9.09E+22	9.09E+22	2.11E+23	2.11E+23	-0.07002	1.3969	1.326884	0.733266	3.266E+01	3.778E+05	3.778E+05
40.41	9	33.776	33.776	0.186	1.351	-4.6427	-0.06959	0.997575	983.5	8.61E+22	8.61E+22	2.11E+23	2.11E+23	-0.06631	1.3967	1.330391	0.694442	2.929E+01	3.578E+05	3.578E+05
40.41	9	33.776	33.776	0.186	1.351	-4.6427	-0.06959	0.997575	982.5	8.15E+22	8.15E+22	2.11E+23	2.11E+23	-0.0628	1.3965	1.333702	0.657673	2.627E+01	3.388E+05	3.389E+05
40.41	9	33.776	33.776	0.186	1.351	-4.6427	-0.06959	0.997575	981.5	7.72E+22	7.72E+22	2.11E+23	2.11E+23	-0.05947	1.3963	1.336827	0.622852	2.357E+01	3.209E+05	3.209E+05
40.41	9	33.776	33.776	0.186	1.351	-4.6427	-0.06959	0.997575	980.5	7.31E+22	7.31E+22	2.11E+23	2.11E+23	-0.05632	1.3961	1.339776	0.589874	2.114E+01	3.039E+05	3.039E+05
40.41	9	33.776	33.776	0.186	1.351	-4.6427	-0.06959	0.997575	979.5	6.92E+22	6.92E+22	2.11E+23	2.11E+23	-0.05334	1.3959	1.342558	0.558642	1.896E+01	2.878E+05	2.878E+05
40.41	9	33.776	33.776	0.186	1.351	-4.6427	-0.06959	0.997575	978.5	6.56E+22	6.56E+22	2.11E+23	2.11E+23	-0.05052	1.3957	1.345182	0.529063	1.700E+01	2.726E+05	2.726E+05
40.41	9	33.776	33.776	0.186	1.351	-4.6427	-0.06959	0.997575	977.5	6.21E+22	6.21E+22	2.11E+23	2.11E+23	-0.04784	1.3955	1.347657	0.501051	1.525E+01	2.582E+05	2.582E+05
40.41	9	33.776	33.776	0.186	1.351	-4.6427	-0.06959	0.997575	976.5	5.88E+22	5.88E+22	2.11E+23	2.11E+23	-0.04531	1.3953	1.34999	0.474522	1.368E+01	2.445E+05	2.445E+05
40.41	9	33.776	33.776	0.186	1.351	-4.6427	-0.06959	0.997575	975.5	5.57E+22	5.57E+22	2.11E+23	2.11E+23	-0.04291	1.3951	1.352189	0.449398	1.227E+01	2.315E+05	2.316E+05
40.41	9	33.776	33.776	0.186	1.351	-4.6427	-0.06959	0.997575	974.5	5.27E+22	5.27E+22	2.11E+23	2.11E+23	-0.04064	1.3949	1.354261	0.425604	1.100E+01	2.193E+05	2.193E+05
40.41	9	33.776	33.776	0.186	1.351	-4.6427	-0.06959	0.997575	973.5	4.99E+22	4.99E+22	2.11E+23	2.11E+23	-0.03849	1.3947	1.356213	0.403069	9.869E+00	2.077E+05	2.077E+05
40.41	9	33.776	33.776	0.186	1.351	-4.6427	-0.06959	0.997575	972.5	4.73E+22	4.73E+22	2.11E+23	2.11E+23	-0.03645	1.3945	1.358051	0.381728	8.852E+00	1.967E+05	1.967E+05
40.41	9	33.776	33.776	0.186	1.351	-4.6427	-0.06959	0.997575	971.5	4.48E+22	4.48E+22	2.11E+23	2.11E+23	-0.03452	1.3943	1.35978	0.361517	7.939E+00	1.863E+05	1.863E+05
40.41	9	33.776	33.776	0.186	1.351	-4.6427	-0.06959	0.997575	970.5	4.24E+22	4.24E+22	2.11E+23	2.11E+23	-0.03269	1.3941	1.361408	0.342376	7.121E+00	1.764E+05	1.764E+05
40.41	9	33.776	33.776	0.186	1.351	-4.6427	-0.06959	0.997575	969.5	4.02E+22	4.02E+22	2.11E+23	2.11E+23	-0.03096	1.3939	1.362939	0.324248	6.387E+00	1.671E+05	1.671E+05
40.41	9	33.776	33.776	0.186	1.351	-4.6427	-0.06959	0.997575	968.5	3.81E+22	3.81E+22	2.11E+23	2.11E+23	-0.02932	1.3937	1.364378	0.30708	5.728E+00	1.582E+05	1.582E+05
40.41	9	33.776	33.776	0.186	1.351	-4.6427	-0.06959	0.997575	967.5	3.6E+22	3.6E+22	2.11E+23	2.11E+23	-0.02777	1.3935	1.365731	0.290821	5.138E+00	1.498E+05	1.498E+05
40.41	9	33.776	33.776	0.186	1.351	-4.6427	-0.06959	0.997575	966.5	3.41E+22	3.41E+22	2.11E+23	2.11E+23	-0.0263	1.3933	1.367001	0.275423	4.608E+00	1.419E+05	1.419E+05
40.41	9	33.776	33.776	0.186	1.351	-4.6427	-0.06959	0.997575	965.5	3.23E+22	3.23E+22	2.11E+23	2.11E+23	-0.02491	1.3931	1.368194	0.26084	4.133E+00	1.344E+05	1.344E+05

x	t	L_o	L	k	omega	s	d	cosh ks	cosh kd	θ	cos θ	P (N/m²)	Area (m²)	Fy (N)
-29.207	9	33.776	33.776	0.186	1.351	965	1000	4.47E+77	3E+80	-17.5915	0.307669	14.73221	8	117.8577
-27.207	9	33.776	33.776	0.186	1.351	965	1000	4.47E+77	3E+80	-17.2195	-0.05922	-2.83579	16	-45.3726
-25.207	9	33.776	33.776	0.186	1.351	965	1000	4.47E+77	3E+80	-16.8475	-0.41801	-20.0159	24	-480.381
-23.207	9	33.776	33.776	0.186	1.351	965	1000	4.47E+77	3E+80	-16.4755	-0.71962	-34.4579	32	-1102.65
-21.207	9	33.776	33.776	0.186	1.351	965	1000	4.47E+77	3E+80	-16.1035	-0.92279	-44.1862	40	-1767.45
-19.207	9	33.776	33.776	0.186	1.351	965	1000	4.47E+77	3E+80	-15.7315	-0.99972	-47.87	40	-1914.8
-17.207	9	33.776	33.776	0.186	1.351	965	1000	4.47E+77	3E+80	-15.3595	-0.9399	-45.0055	32	-1440.17
-15.207	9	33.776	33.776	0.186	1.351	965	1000	4.47E+77	3E+80	-14.9875	-0.7515	-35.9844	24	-863.625
-13.207	9	33.776	33.776	0.186	1.351	965	1000	4.47E+77	3E+80	-14.6155	-0.4603	-22.0408	16	-352.652
-11.207	9	33.776	33.776	0.186	1.351	965	1000	4.47E+77	3E+80	-14.2435	-0.10613	-5.08208	8	-40.6567
											Summatior	-242.746	240	-7889.9

x	t	L_o	L	k	s	d	omega	cosh ks	cosh kd	θ	cos θ	P (N/m^2)	Area (m^2)	Fy (N)
31.414	9	33.776	33.776	0.186	1.351	1000	1.85378	1.031739	3E+80	-10.841	-0.15394	-1.8E-77	8	-1.4E-76
33.414	9	33.776	33.776	0.186	1.351	1000	1.85378	1.031739	3E+80	-10.469	-0.50256	-5.7E-77	16	-9.2E-76
35.414	9	33.776	33.776	0.186	1.351	1000	1.85378	1.031739	3E+80	-10.097	-0.78243	-8.9E-77	24	-2.1E-75
37.414	9	33.776	33.776	0.186	1.351	1000	1.85378	1.031739	3E+80	-9.72502	-0.95527	-1.1E-76	32	-3.5E-75
39.414	9	33.776	33.776	0.186	1.351	1000	1.85378	1.031739	3E+80	-9.35302	-0.99743	-1.1E-76	40	-4.5E-75
41.414	9	33.776	33.776	0.186	1.351	1000	1.85378	1.031739	3E+80	-8.98102	-0.90314	-1E-76	40	-4.1E-75
43.414	9	33.776	33.776	0.186	1.351	1000	1.85378	1.031739	3E+80	-8.60902	-0.68532	-7.8E-77	32	-2.5E-75
45.414	9	33.776	33.776	0.186	1.351	1000	1.85378	1.031739	3E+80	-8.23702	-0.37374	-4.3E-77	24	-1E-75
47.414	9	33.776	33.776	0.186	1.351	1000	1.85378	1.031739	3E+80	-7.86502	-0.01104	-1.3E-78	16	-2E-77
49.414	9	33.776	33.776	0.186	1.351	1000	1.85378	1.031739	3E+80	-7.49302	0.353175	4.02E-77	8	3.22E-76
											Summatior	-5.7E-76	240	-1.9E-74

x [m]	z	ηw	h	h	omega	kbeta	sin theta	cos theta	N	kwh kp	kwh ko	kwh kd	kbh kd	u[x] water particle	u[x] current	total u[x]	a[x] water particle	a[x]	a[x] [m/s²]	a[z] water p	[m/s²]	dx [N/m]	dz [N/m]	dy [N/m]	total horizontal force[x] [N/m]	F-dx [N/m]	F-dz [N/m]	F-dy [N/m]	total horizontal force[y] [N/m]
-20.207	0	33.776	33.776	0.186	1.351	-3.7585	-0.81567	0.578517	965	4.47184E+77	4.47184E+77	3.0043E+80	3.0043E+80	-0.002838869	1.393	1.390161	0.002013477	1.390163	0.001471	-0.00207	12875.61	758.0157	13633.63002	-19.2126	-1068.751	-1087.963204

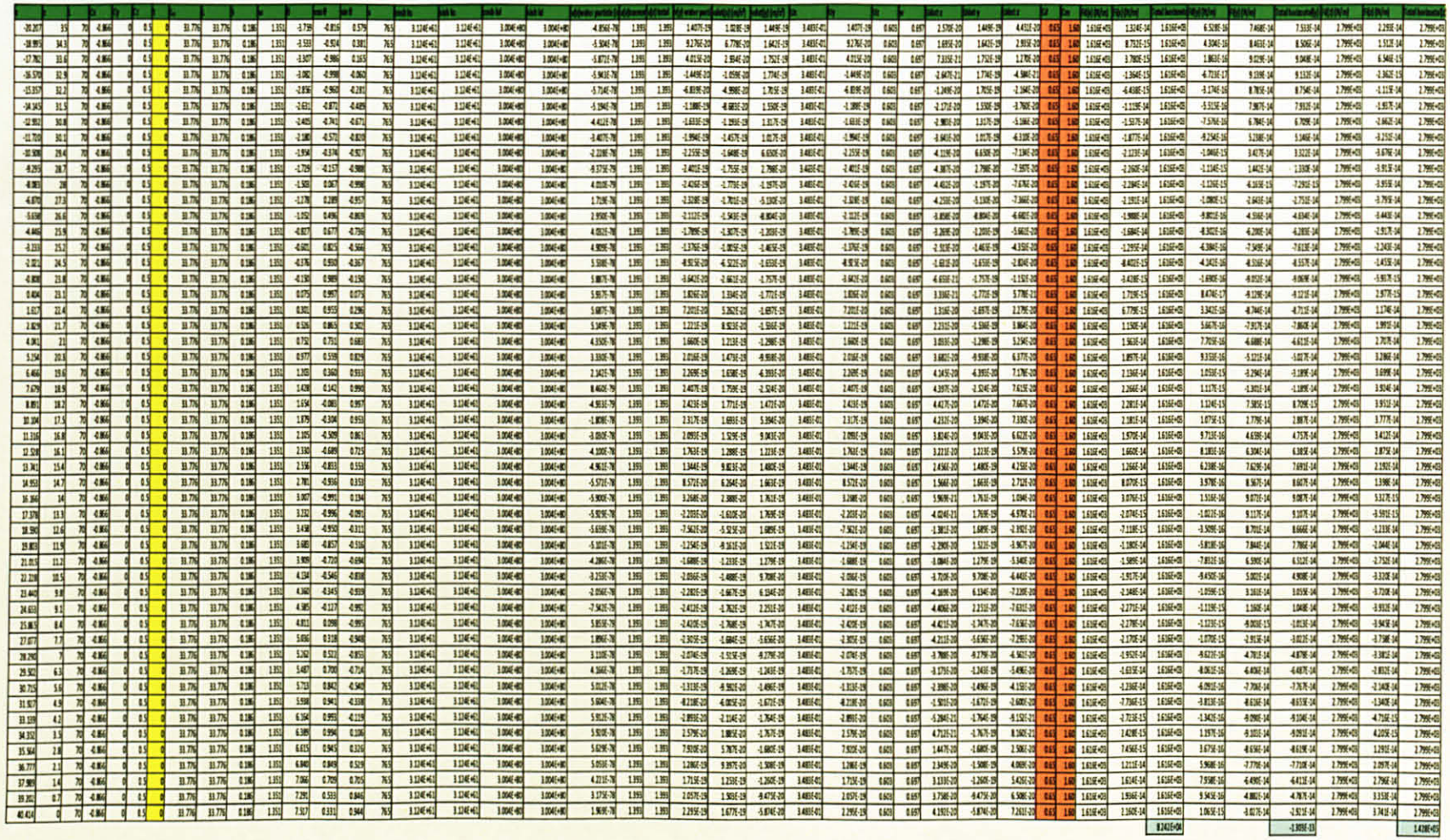

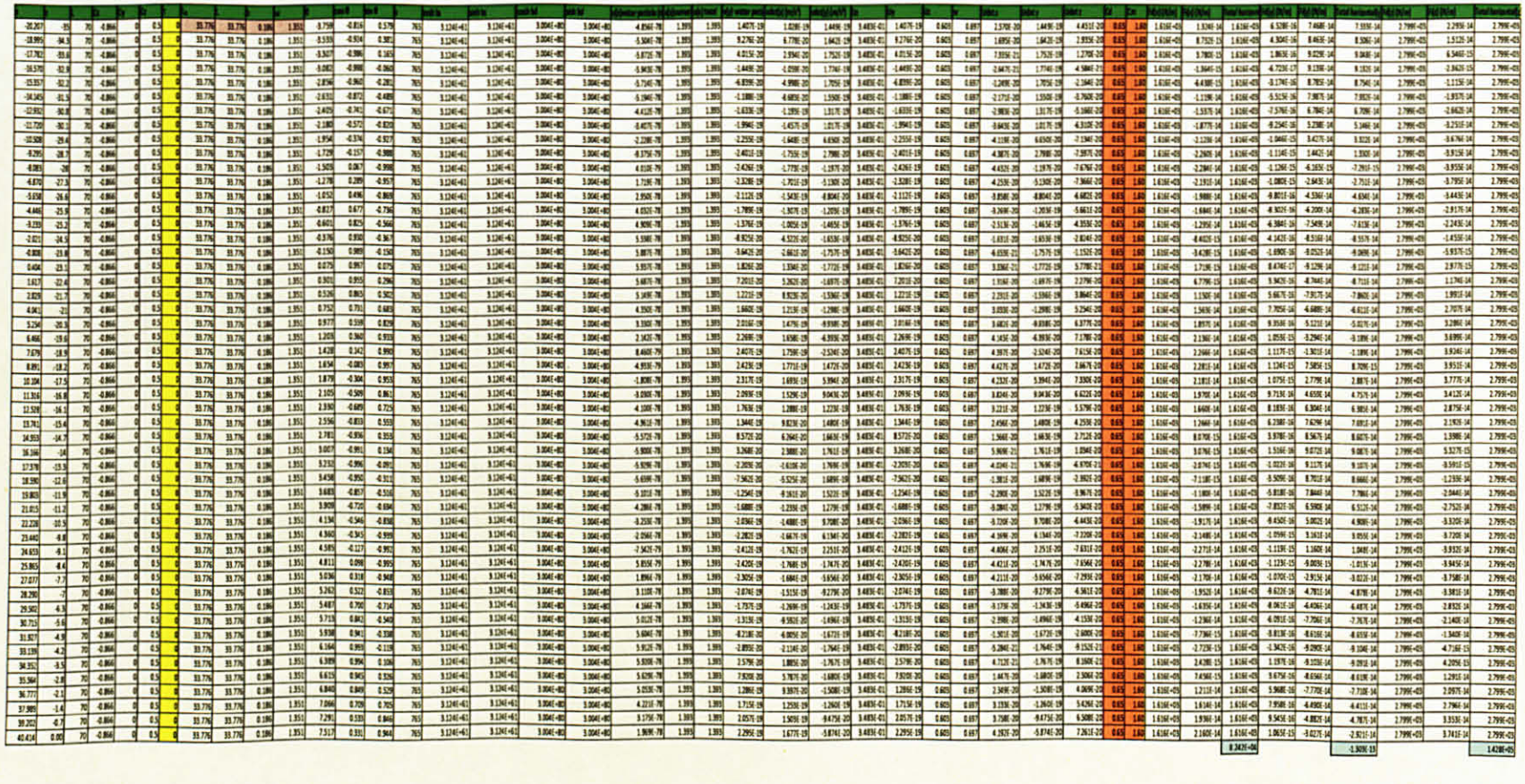

t	Fx (N/m)	Fy(N)
0	29,386,670.875	-10,408.578
1	24,189,830.315	6,239.436
2	-17,913,291.079	15,879.725
3	-41,196,321.273	685.104
4	5,355,419.239	-15,580.978
5	34,201,931.565	-7,479.372
6	10,727,265.510	12,319.510
7	-29,019,056.247	12,851.438
8	-22,540,423.671	-6,715.490
9	2,639,064.391	-15,779.806

t	Fx (N/m)	Fy (N/m)	Fz (N/m)
0	846,530.864	-54,398.160	285,501.815
1	872,928.538	25,794.763	285,501.815
2	802,888.991	65,650.893	285,501.815
3	745,946.040	2,832.280	285,501.815
4	791,159.328	-64,410.240	285,501.815
5	867,813.845	-30,919.680	285,501.815
6	856,029.909	50,931.546	285,501.815
7	774,235.200	53,130.732	285,501.815
8	750,351.363	-27,761.854	285,501.815
9	821,733.335	-65,232.143	285,501.815

t	Fx (N/m)	Fy(N)	Fz (N/m)	
0	30,233,201.739	-64,806.738	285,535.492	
1	25,062,758.853	32,034.199	285,490.212	
2	-17,110,402.088	81,530.619	285,450.854	
3	40,450,375.233	3,517.384	285,437.510	
4	6,146,578.567	-79,991.218	285,456.990	
5	35,069,745.410	-38,399.052	285,499.351	
6	11,583,295.418	63,251.056	285,542.970	
7	-28,244,821.046	65,982.170	285,565.581	
8	-21,790,072.308	-34,477.344	285,555.643	
9	3,460,797.726	-81,011.949	285,518.228	TOTAL ALL

(C x omega)^2	(K-(m x (omega^2)))^2	(u + v)^0.5	F/ (H/2)	(X/W)
318888197.7	7.18715E+12	2680944.61	14563893373	5432.373842
625020805	3.04029E+13	5513935.388	165682631.3	30.04798201
1033197967	8.63265E+13	9291262.339	149269287.3	16.06555512
1543418568	1.9636E+14	14012913.96	133683947.3	9.540053387
2869995214	6.91121E+14	26289237.61	116713296.9	4.439584696
2869995214	6.91121E+14	26289237.61	91491020.58	3.480170173
3686344985	1.1454E+15	33843851.4	87447757.97	2.58385953
4604741891	1.79291E+15	42342823.56	69320525.04	1.637125709
5625187245	2.6818E+15	51786166.22	52169821	1.007408441
6747677637	3.86558E+15	62173847.83	71694905.66	1.153136056
7972204942	5.40309E+15	73505793.18	55386440.58	0.753497625
9298780868	7.35856E+15	85782110.61	76070127.23	0.886783115
10727404334	9.80154E+15	99002790.14	86693211.48	0.875664326
12258061952	1.28069E+16	113167707.8	84524546.08	0.746896334
13890770169	1.6455E+16	128277016	73400513.45	0.572203157
15625520124	2.08313E+16	144330632.4	73522993.9	0.509406719
17462320325	2.60269E+16	161328636	50791481.66	0.3148324
19401158918	3.2138E+16	179270917.1	61270767.22	0.341777508
21442031692	3.92663E+16	198157436.6	68943856.93	0.347924651
23584999403	4.75191E+16	217988756.7	80900750.47	0.3711235
25829995673	5.70083E+16	238764263.4	75828494.99	0.317587288
28176949878	6.78515E+16	260483302.8	67978290.29	0.260969857
30626062320	8.01726E+16	283147728.8	40301603.57	0.142334193
33177104864	9.40989E+16	306755430	61526628.68	0.200572256
35830181151	1.09765E+17	331307365.7	81318146.04	0.245446237
38585549092	1.2731E+17	356805922.4	78250622.55	0.219308643
41442755759	1.46878E+17	383246908.9	72166900.7	0.188303934
44402005968	1.68619E+17	410632220.5	40299278.46	0.098139592

T	F	f	S(f)	ω
40	7,281,946,686.284	0.025	1	0.15708
28.5714286	82,841,315.654	0.035	1	0.219911
22.2222222	74,634,643.645	0.045	1	0.282743
18.1818182	66,841,973.656	0.055	1	0.345575
15.3846154	58,356,648.469	0.065	1	0.471239
13.3333333	45,745,510.292	0.075	1	0.471239
11.7647059	43,723,878.984	0.085	1	0.534071
10.5263158	34,660,262.519	0.095	1	0.596902
9.52380952	26,084,910.498	0.105	1	0.659734
8.69565217	35,847,452.832	0.115	1	0.722566
8	27,693,220.289	0.125	1	0.785398
7.40740741	38,035,063.615	0.135	1	0.84823
6.89655172	43,346,605.738	0.145	1	0.911062
6.4516129	42,262,273.039	0.155	1	0.973894
6.06060606	36,700,256.727	0.165	1	1.036726
5.71428571	36,761,496.949	0.175	1	1.099557
5.40540541	25,395,740.831	0.185	1	1.162389
5.12820513	30,635,383.610	0.195	1	1.225221
4.87804878	34,471,928.465	0.205	1	1.288053
4.65116279	40,450,375.233	0.215	1	1.350886
4.44444444	37,914,247.494	0.225	1	1.413718
4.25531915	33,989,145.144	0.235	1	1.476548
4.08163265	20,150,801.787	0.245	1	1.539381
3.92156863	30,763,314.339	0.255	1	1.602212
3.77358491	40,659,073.020	0.265	1	1.665042
3.63636364	39,125,311.277	0.275	1	1.727878
3.50877193	36,083,450.350	0.285	1	1.790709
3.38983051	20,149,639.229	0.295	1	1.85354

f	RAO	S(f)	S(f)Surge
0.055	9.540053	4.75E-05	0.004322
0.065	4.439585	0.076127	1.500451
0.075	3.48017	1.607817	19.47322
0.085	2.58386	5.864972	39.15649
0.095	1.637126	9.717513	26.04469
0.105	1.007408	11.00358	11.16722
0.115	1.153136	10.2822	13.67248
0.125	0.753498	8.702447	4.94089
0.135	0.886783	7.001984	5.50625
0.145	0.875664	5.497776	4.215629
0.155	0.746896	4.27414	2.384347
0.165	0.572203	3.317148	1.086089
0.175	0.509407	2.581943	0.670002
0.185	0.314832	2.020751	0.200296
0.195	0.341778	1.592417	0.186013
0.205	0.347925	1.264328	0.153049
0.215	0.371124	1.011616	0.139333
0.225	0.317587	0.815657	0.082269
0.235	0.26097	0.662604	0.045127
0.245	0.142334	0.542169	0.010984
0.255	0.200572	0.446698	0.01797
0.265	0.245446	0.370463	0.022318
0.275	0.219309	0.309158	0.014869
0.285	0.188304	0.259525	0.009202
0.295	0.09814	0.219079	0.00211